BIOCHEMISTRY
including biophysical chemistry & molecular biology
Article

Biochemistry **2009,** *48,* 8343–8354 8343
DOI: 10.1021/bi900849z

Conformational Heterogeneity and Spin-Labeled −SH Groups: Pulsed EPR of Na,K-ATPase[†]

R. Guzzi,[‡] R. Bartucci,[‡] L. Sportelli,[‡] M. Esmann,[§] and D. Marsh*,[∥]

[‡]*Dipartimento di Fisica and UdR CNISM, Università della Calabria, 87036 Arcavacata di Rende (CS), Italy,* [§]*Department of Physiology and Biophysics, Aarhus University, Aarhus, Denmark, and* [∥]*Max-Planck-Institut für biophysikalische Chemie, Abt. Spektroskopie, 37077 Göttingen, Germany*

Received May 19, 2009; Revised Manuscript Received July 29, 2009

ABSTRACT: Membranous Na,K-ATPase from shark salt gland and from pig kidney was spin-labeled on class I −SH groups in the presence of glycerol, or on class II −SH groups in the absence of glycerol. The class I-labeled preparations retain full enzymatic activity, whereas the class II-labeled preparations are at least partially inactivated. This provides an excellent testbed on which to demonstrate how advanced electron paramagnetic resonance (EPR) can provide novel information on specific residues in unique environments in a complex, membrane-bound transport system. The polarity of the environment, and the librational dynamics and conformational exchange, of the spin-labeled groups were studied with pulsed EPR by using electron spin echo envelope modulation (ESEEM) spectroscopy and spin−echo detected (ED) EPR spectroscopy, respectively. ^{2}H-ESEEM spectra of membranes dispersed in D_2O reveal that class I groups of the shark enzyme are more exposed to water than are those of the pig enzyme or class II groups of either species, consistent with the more superficial membrane location in the former case. Spin−echo decay curves indicate conformational heterogeneity at low temperatures (< 150 K), but a more homogeneous conformational state at higher temperatures that is characterized by a single phase-memory T_{2M} relaxation time. Conventional EPR lineshapes also demonstrate conformational microheterogeneity at low temperatures: the inhomogeneously broadened lines narrow progressively with increasing temperature reaching an almost pure Lorentzian line shape at temperatures of ca. 220 K and above. The inhomogeneous broadening at low temperature is well described by a Gaussian distribution of Lorentzian lines. ED spectra as a function of echo-delay time demonstrate the onset of rapid librational motions of appreciable amplitude, and slower conformational exchange, at temperatures above 220 K. These motions could drive transitions between the different conformational substates, which are frozen in at lower temperatures but contribute to the pathways between the principal enzymatic intermediates at higher temperatures.

The sodium pump is a membrane-bound Na,K-ATPase enzyme that is responsible for maintaining the ionic balance in animal cells. The transmembrane section of the protein consists of 10 transmembrane helices from the α-subunit and a single transmembrane helix of the *β*-subunit. The α-subunit has a large cytoplasmic domain that bears the enzymatic active site (*1*). The protein contains 23 cysteine residues in the α-subunit which are conserved between pig and shark (see Figure 1). Several of these cysteines are amenable to chemical modification by spin-label probes (*2*) that may be used to investigate the local environment and the conformational states of the protein.

Previously, we have classified the −SH groups of the Na,K-ATPase from shark salt gland as follows: a number of groups (class I, approximately two per α-subunit) can be reacted with *N*-ethyl maleimide (NEM)[1] in the presence of glycerol or sucrose with no effect on the overall or partial reactions of the enzyme. In addition to these groups, approximately 5 groups per α-subunit can be modified with NEM in the absence of glycerol: these are termed class II groups (*3*, *4*). Modification of these class II groups leads to loss of Na,K-ATPase activity. One of the class II groups can be protected from modification with NEM by ATP in the presence of K^+. In this case, the enzyme retains the ability to phosphorylate from ATP, but the affinity for K^+ is reduced drastically, which leads to loss of overall Na,K-ATPase activity (*5*−*7*). The catalytic α-subunit of the Na,K-ATPase from pig has ca. 94% homology with the shark enzyme: only 60 residues, none of them cysteines, are nonhomologous.

In the present work, we investigate the various spin-labeled preparations of Na,K-ATPase from shark salt gland and pig kidney by a combination of different pulsed EPR techniques (see, e.g., ref *8*) and conventional EPR spectroscopy. The previous detailed characterization of −SH groups in Na,K-ATPase provides an excellent testbed on which to demonstrate how these advanced EPR techniques can be used to provide novel information about specific residues in unique environments such as those in a complex membrane-bound transport system. ESEEM spectroscopy of membranes dispersed in D_2O is used to study the exposure of the groups and their interaction with water. Spin−echo decay curves and fitting of the conventional lineshapes are used to study the conformational microheterogeneity

[†]We thank the Aarhus University Research Foundation for financial support.

*Corresponding author. Tel: +49-551 201 1285; Fax: +49-551 201 1501. E-mail: dmarsh@gwdg.de.

[1]Abbreviations: NEM, *N*-ethyl maleimide; 5-MSL, 3-maleimido-1-oxyl-2,2,5,5-tetramethylpyrrolidine; CDTA, *trans*-1,2-cyclohexylenedinitrilotetraacetic acid; SDS, sodium dodecyl sulfate; EPR, electron paramagnetic resonance; ESEEM, electron spin echo envelope modulation; ED, echo detected; HSA, human serum albumin.

Published on Web 07/30/2009

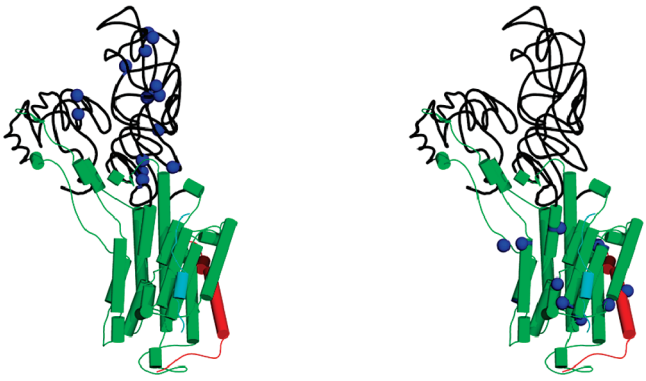

FIGURE 1: Location of cysteine residues (blue balls) in the α-subunit of Na,K-ATPase from pig kidney (*1*). Left panel, extramembranous part (14 cysteines); right panel, intramembranous part (9 cysteines). In green are the α-subunit peptides that remain membrane-associated after trypsinization in the presence of Rb^+; the parts removed by trypsin are indicated in black (*34*). The membrane-spanning domain of the *β*-subunit is shown in red, and a fragment of the *γ*-subunit is indicated in cyan.

of the protein at low temperature and the averaging that takes place by thermal fluctuations at higher temperatures. Such studies, by other techniques, have previously been restricted to relatively small, soluble proteins (*9*, *10*). The present work therefore further extends our knowledge of conformational substates to large, membrane-spanning active-transport proteins. ED spectra as a function of echo-delay time are used to study the onset of rapid librational motions, and conformational exchange on different time scales, and to correlate this with the thermal averaging of conformational substates that may lie on the pathway of the enzymatic cycle.

MATERIALS AND METHODS

Enzyme Preparation. The Na,K-ATPase membranes from pig kidney and shark salt gland were prepared as described earlier (*11*, *12*). Pig kidney microsomal membranes were prepared as outlined in ref *11*, treated with SDS (*13*), and purified by differential centrifugation to a specific activity of 28 *μ*mol of P_i per mg of protein per min at 37 °C (see ref *11* for experimental details). Shark salt gland microsomal membranes were prepared as outlined in ref *12*, treated with deoxycholate (omitting saponin) and purified by differential centrifugation to a specific activity of 32 *μ*mol of P_i per mg of protein per min at 37 °C (see ref *12* for experimental details). The shark enzyme was stored at a protein concentration of about 5 mg/mL in 20 mM histidine and 25% glycerol (pH 7.0), and the pig kidney enzyme was stored at a protein concentration of about 4 mg/mL in 20 mM histidine, 250 mM sucrose and 1 mM EDTA (pH 7.0). The α- and *β*-subunits of the Na,K-ATPase have molecular weights of 112 kDa and 35.5 kDa, respectively, for both species; these subunits constitute 70% of the total protein of the shark preparation and 60−70% of that from pig kidney. Protein concentrations were determined using the Lowry method (*14*), and enzymatic assays were performed as described previously (*15*).

Prelabeling of Na,K-ATPase −SH groups with NEM. Prelabeling of shark Na,K-ATPase with NEM to block class I −SH groups was performed as follows (see ref *4* for details): Na,K-ATPase (approximately 1 mg/mL) was incubated at 20 °C with 0.1 mM NEM in 30 mM histidine (pH 7.0 at 23 °C)/5 mM CDTA/150 mM KCl and 36% (v/v) glycerol for 60 min. The reaction was stopped by addition of an equal volume of 20 mM histidine (pH 7.0 at 20 °C) and 10% (v/v) glycerol containing 1 mM 2-mercaptoethanol, and the membranes were pelleted at 200000*g*. The membranes were washed twice by centrifugation in 20 mM histidine (pH 7.0 at 20 °C) and 25% (v/v) glycerol at 200000*g*. The prelabeled enzyme had more than 95% of the initial specific activity and was stored in 20 mM histidine and 25% (v/v) glycerol at −20 °C.

Prelabeling of pig Na,K-ATPase followed the same route: Na,K-ATPase (approximately 1 mg/mL) was incubated at 20 °C with 10 mM NEM in 30 mM histidine (pH 7.0 at 23 °C)/5 mM CDTA/150 mM KCl and 36% (v/v) glycerol for 60 min. The reaction was stopped by addition of an equal volume of 20 mM histidine (pH 7.0 at 20 °C) and 10% (v/v) glycerol containing 12 mM 2-mercaptoethanol, and the membranes were pelleted at 200000*g*. The membranes were washed twice by centrifugation in 20 mM histidine, 250 mM sucrose and 1 mM EDTA (pH 7.0) at 200000*g*. The prelabeled enzyme had more than 90% of the initial specific activity and was stored at −20 °C in 20 mM histidine, 250 mM sucrose and 1 mM EDTA (pH 7.0).

Spin-Labeling of Na,K-ATPase Membranes. (*a*) *Maleimide Spin-Labeling of Class I Groups*. Class I −SH groups in the Na,K-ATPase membranes were spin-labeled with 5-MSL (Sigma, St. Louis, MO) by using the same experimental protocol as given above for prelabeling with NEM. For shark enzyme, the native membranes were treated with 0.2 mM 5-MSL (added from a 100 mM stock solution in ethanol), and the spin-labeled enzyme had more than 95% of the initial specific activity. For pig enzyme, a spin-label concentration of 1.25 mM was used, and the spin-labeled enzyme had more than 90% of the initial specific activity.

(*b*) *Maleimide Spin-Labeling of Class II Groups*. Selective spin-labeling of the class II −SH groups, which are essential for the overall Na,K-ATPase activity, was performed as follows (*3*): Na,K-ATPase prelabeled with NEM (see above) was incubated for 60 min with 5-MSL at 37 °C in 30 mM histidine (pH 7.4 at 37 °C) in the presence of 150 mM KCl/5 mM CDTA/3 mM ATP (Tris salt). For shark enzyme, the final 5-MSL concentration was 0.125 mM (with a residual specific activity of 8%), and for pig, 1.0 mM 5-MSL was used resulting in a residual activity of 20%. For both enzymes, the reaction was stopped by addition of 1 mM 2-mercaptoethanol, and the membranes were pelleted by centrifugation in 25% glycerol (as described for the prelabeling procedure, see above). The membranes were then washed twice (see above).

Deuterium Exchange of Spin-Labeled Membranes. A buffer was prepared by using D_2O containing the following salts: 11 mM Tris, 11 mM Na_3CDTA and 22 mM NaCl (pH 7.0 at 20 °C). 5-MSL spin-labeled Na,K-ATPase (see above) was pelleted by centrifugation, and approximately 15 mg of protein was homogenized in 10 mL of the D_2O buffer. This membrane suspension was incubated at 14 °C for 60 min and pelletted by centrifugation at 100000*g* for 2 h at 14 °C. The pellet was homogenized in 10 mL of the D_2O buffer and incubated at 14 °C for 12 h, after which it was pelleted by centrifugation as above. The pellets were transferred to quartz EPR tubes (inner diameter 3 mm) with a total sample volume of about 100 *μ*L and a membrane protein concentration of approximately 40 mg/mL. The EPR samples were stored at −20 °C prior to measurement.

EPR Spectroscopy. Pulsed EPR data were collected on an ELEXSYS E580 9-GHz Fourier transform FT-EPR spectrometer (Bruker, Germany) equipped with a MD5 dielectric resonator and a CF 935P cryostat (Oxford Instruments, U.K.).

To obtain ESEEM spectra, three-pulse, stimulated echo ($\pi/2-\tau-\pi/2-T-\pi/2-\tau-$echo) decays were collected by using microwave pulse widths of 12 ns, with the microwave power adjusted to give $\pi/2$-pulses. The time delay T between the second and the third pulses was incremented from 20 ns by 700 steps of $\Delta T = 12$ ns, while maintaining the separation τ between the first and the second pulses constant at 168 ns. A four-step phase-cycling program, $+(x,x,x)$, $-(x,-x,x)$, $-(-x,x,x)$, $+(-x,-x,x)$, where the initial sign indicates the phase of the detection ($\pm y$), was used to eliminate unwanted echoes. The magnetic field was set to the maximum of the EPR absorption. The time-dependent echo amplitudes, $V(\tau,T)$, were processed to yield standardized ESEEM intensities, according to the protocol developed previously (*16*, *17*). The average experimental echo decay, $\langle V(\tau,T)\rangle$, was fitted with a biexponential function. The normalized ESE modulation signal was then obtained as

$$V_{\mathrm{norm}}(\tau,T) = V(\tau,T)/\langle V(\tau,T)\rangle - 1 \qquad (1)$$

Three levels of zero-filling were added at the end of the data to increase the total number of points to 4K. The absolute-value ESEEM spectrum was then calculated, with specific inclusion of the dwell time ($\Delta T = 12$ ns) between points, yielding standardized intensities with dimensions of time (*17*).

Two-pulse ($\pi/2-\tau-\pi-\tau-$echo) spin−echo decays were obtained by integrating the echo and incrementing the pulse spacing, τ. The window for the integration was 160 ns. The microwave pulse widths were 32 and 64 ns, with the microwave power adjusted to provide $\pi/2$ and π-pulses, respectively. Use of softer pulses than those employed for recording the ESEEM spectra, and integration of the echo, largely suppresses the proton hyperfine modulations from preparations in H_2O buffer. The magnetic field was again set to the EPR absorption maximum. The τ-dependence of the integrated echo intensity, $I(\tau)$, was fitted with a double exponential decay function:

$$I(\tau) = I_1(0)\exp(-2\tau/T_{2\mathrm{M},1}) + I_2(0)\exp(-2\tau/T_{2\mathrm{M},2}) \qquad (2)$$

where $T_{2\mathrm{M},i}$ are the phase-memory times of the different components and $I_i(0)$ are their respective intensities.

Two-pulse ($\pi/2-\tau-\pi-\tau-$echo) echo-detected EPR spectra were obtained by recording the integrated spin−echo signal at fixed interpulse delay τ, while sweeping the magnetic field. The integration window and the microwave pulse widths were the same as those used for recording the echo decays. The original ED spectra, $\mathrm{ED}_T(2\tau,H)$, were corrected for instantaneous spin diffusion by normalizing with respect to those recorded at 77 K, where no molecular motion is expected. The corrected spectra, $\mathrm{ED}_T^{\mathrm{corr}}(2\tau,H)$, recorded at temperature T are plotted as a function of magnetic field, H, according to ref *18*:

$$\mathrm{ED}_T^{\mathrm{corr}}(2\tau,H) = \mathrm{ED}_T(2\tau,H)\frac{\mathrm{ED}_{77K}(2\tau_0,H)}{\mathrm{ED}_{77K}(2\tau,H)} \qquad (3)$$

where τ_0 is the shortest value of τ for which ED spectra were obtained. Relaxation rates, $W(H,\tau_1,\tau_2)$, were determined from the ratio of corrected ED spectra recorded at two different values, τ_1 and τ_2, of the interpulse delay by using the following relation (*19*):

$$W(H,\tau_1,\tau_2) = \ln\left[\frac{\mathrm{ED}(2\tau_1,H)}{\mathrm{ED}(2\tau_2,H)}\right]\cdot\frac{1}{2(\tau_2-\tau_1)} \qquad (4)$$

where $\mathrm{ED}(2\tau,H)$ is the ED spectral lineheight at field position H. These relaxation rates are averaged over the time interval from τ_1 to τ_2, and are characterized by the maximum values, W_{L} and W_{H}, determined in the low- and high-field regions, respectively, of the ED spectra. Calibration of the W_{L} and W_{H} relaxation rates in terms of the amplitude-correlation time product, $\langle\alpha^2\rangle\tau_c$, of rotational motion from small-amplitude librations is taken from the results of spectral simulations (*18*−*20*). Here, α is the angular amplitude, τ_c is the correlation time, and angular brackets indicate an average over the librational motion.

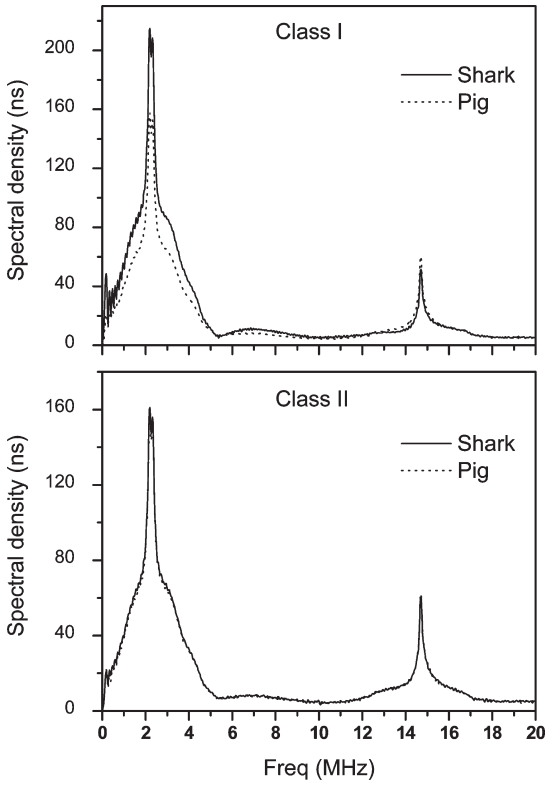

FIGURE 2: Absolute-value Fourier transform ESEEM spectra of Na,K-ATPase membranes from shark salt gland (solid lines) and pig kidney (dotted lines) that are labeled on class I (upper panel) or class II (lower panel) −SH groups with the 5-MSL maleimide spin label. Membranes are dispersed in D_2O buffer. ESEEM intensities are standardized as described in Materials and Methods.

Three-pulse ($\pi/2-\tau-\pi/2-T-\pi/2-\tau-$echo) stimulated echo-detected EPR spectra, $\mathrm{ED}_{\mathrm{SE}}(T,H)$, were obtained by recording the integrated spin−echo signal at fixed interpulse delays τ and T, while sweeping the magnetic field. Corresponding inversion recovery ($\pi-T-\pi/2-\tau-\pi-\tau-$echo) echo-detected EPR spectra, $\mathrm{ED}_{\mathrm{IR}}(T,H)$, were obtained in a similar manner. In each case, the integration window and the microwave pulse widths were the same as those used for the two-pulse $\mathrm{ED}(2\tau,H)$ spectra. The original stimulated ED spectra were corrected for spin−lattice relaxation by using the inversion recovery ED spectra (*18*):

$$\mathrm{ED}_{\mathrm{SE}}^{\mathrm{corr}}(T,H) = \mathrm{ED}_{\mathrm{SE}}(T,H)\frac{\Delta\mathrm{ED}_{\mathrm{IR}}(0,H)}{\Delta\mathrm{ED}_{\mathrm{IR}}(T,H)} \qquad (5)$$

where $\Delta\mathrm{ED}_{\mathrm{IR}}(T,H) = \mathrm{ED}_{IR}(\infty,H) - \mathrm{ED}_{\mathrm{IR}}(T,H)$. The spectrum for $T=\infty$ was obtained with the first pulse turned off and, for $T=0$, we take $\mathrm{ED}_{\mathrm{IR}}(0,H) = -\mathrm{ED}_{\mathrm{IR}}(\infty,H)$. Using long π-pulses (120 ns) in the inversion recovery experiment was found to have little effect on the corrected stimulated echo-detected EPR, relative to using shorter π-pulses (32 ns).

Conventional CW EPR spectra were recorded on an ESP-300 9-GHz spectrometer (Bruker, Karlsruhe, Germany) using 100 kHz field modulation; the spectrometer was equipped with

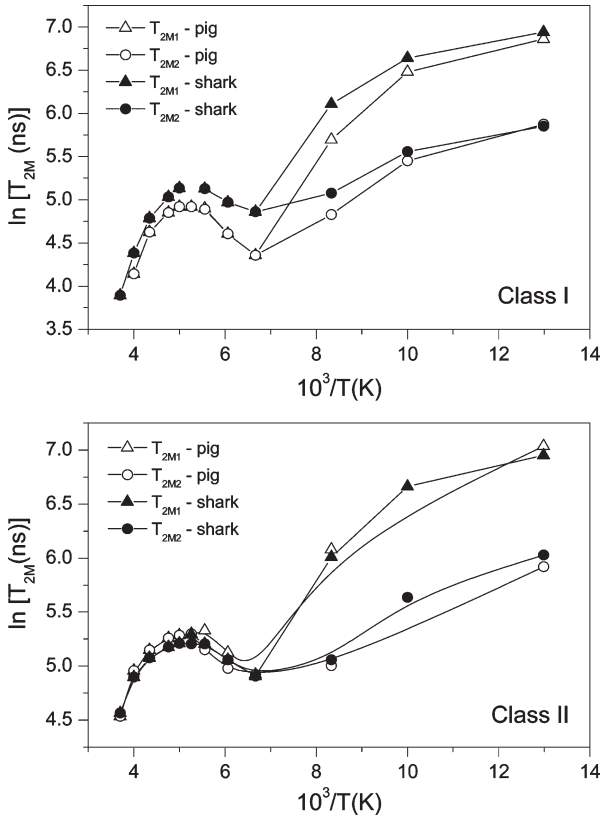

FIGURE 3: Temperature dependence of the phase-memory time, T_{2M}, for 5-MSL-labeled class I (upper panel) or class II (lower panel) −SH groups of shark (solid symbols) and pig (open symbols) Na,K-ATPase. Circles and triangles are from double-exponential fits (eq 2) to the echo decay curves.

an ER 4111 VT temperature controller. The low-field ($m_I = +1$) hyperfine extremum in the CW-EPR powder patterns from random membrane dispersions was fitted by nonlinear least-squares minimization with a Voigt absorption line shape:

$$v(H) = A \int_{-\infty}^{\infty} \frac{\exp(-(H' - H_o)^2/2\Delta H_G^2)}{(\Delta H_L/2)^2 + (H - H')^2}\, dH' \qquad (6)$$

where ΔH_L is the half-width at half-height of each Lorentzian component, ΔH_G is the width of the Gaussian distribution of Lorentzian components, and H_o is the center of the Gaussian distribution. The high-field wings of the $m_I = +1$ hyperfine extrema were omitted from the fitting procedure in order to eliminate any distortion by the powder pattern envelope.

RESULTS

D_2O ESEEM Spectra. The ESEEM spectra of shark and pig Na,K-ATPase samples that are spin-labeled on class I or class II −SH groups with 5-MSL and suspended in D_2O buffer are shown in Figure 2. In all cases, the spectra consist of a peak at the ^{2}H-Larmor frequency of ca. 2.6 MHz that arises from D_2O in the vicinity of the spin-labeled groups and a peak at the ^{1}H-Larmor frequency of 14.6 MHz that arises from matrix protons and serves as an additional internal standard for the D_2O intensity. The D_2O peak consists of a broad component that arises from D_2O molecules that are hydrogen-bonded to the nitroxide and a narrow component that corresponds to D_2O molecules located more remotely from the spin-label site (*16*). The height of the broad component is 40% that of the total, for all samples. It is seen in the upper panel of Figure 2 that the ^{2}H-ESEEM intensity

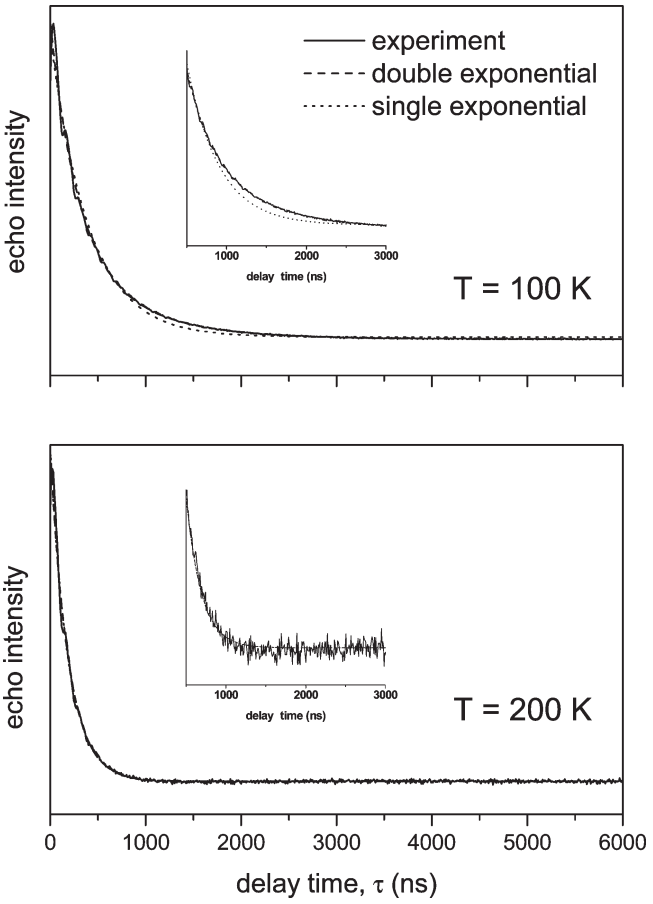

FIGURE 4: Decay of echo amplitude as a function of echo delay time, τ, for 5-MSL-labeled class II −SH groups of shark Na,K-ATPase at 100 K (upper panel) and 200 K (lower panel). Dashed lines are a double exponential fit and dotted lines a single exponential fit to the echo decay curves.

of the shark enzyme is considerably larger than that of the pig enzyme, showing that the class I groups of the former are more exposed to water than are those of the latter. In the lower panel of Figure 2, however, the ESEEM spectra from shark and pig preparations are virtually superimposable, indicating that, on average, the environments of the class II −SH groups are of a similar polarity in the two species.

The total normalized ^{2}H-ESEEM intensity of shark class I groups is intermediate between that of 5-MSL bound covalently at the surface of human serum albumin (HSA) with $I_{tot} = 240$ ns, and that found for a spin label on the 16-C atom of stearic acid, which is bound only shallowly within the hydrophobic association site on HSA with $I_{tot} = 180$ ns (*20*). On the other hand, the total ^{2}H-ESEEM intensities of shark and pig class II groups, as well as that of pig class I groups, which are all very similar, are comparable to that of a spin label on the 12-C atom of stearic acid bound to HSA ($I_{tot} = 150$ ns). The latter has an intermediate exposure to water, because the ^{2}H-ESEEM intensity of the buried 7-C atom of stearic acid bound to HSA is only $I_{tot} = 105$ ns (*20*). The differential exposure of shark class I and class II groups to water is therefore reflected directly by D_2O-ESEEM spectroscopy.

Echo Decay Curves and Phase-Memory Time. Figure 3 shows the temperature dependence of the phase-memory time T_{2M} for Na,K-ATPase preparations labeled on class I (upper panel) or class II (lower panel) −SH groups with 5-MSL and suspended in H_2O buffer. These values were obtained by fitting the experimental echo decay curves with eq 2 for a double

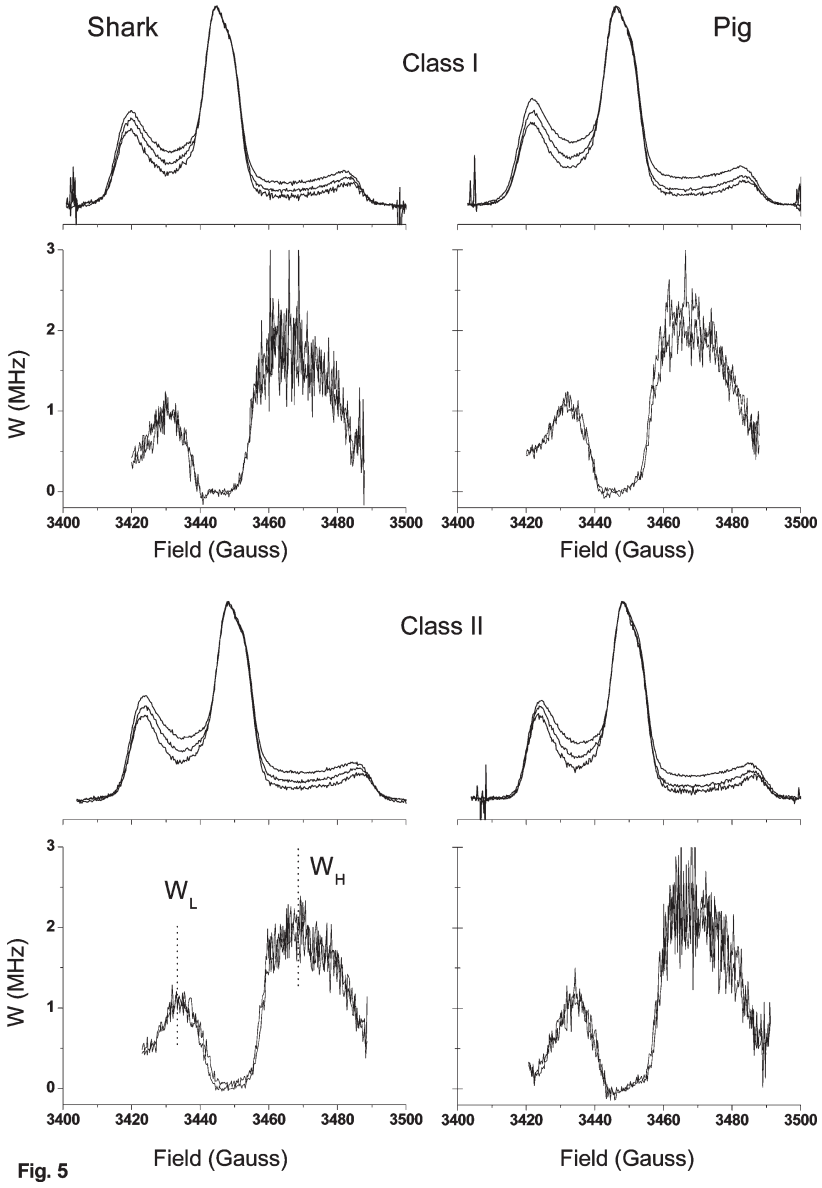

FIGURE 5: Two-pulse, echo-detected EPR spectra of Na,K-ATPase membranes from shark salt gland (left-hand side) and pig kidney (right-hand side) that are labeled on class I (upper panel) or class II (lower panel) −SH groups with the 5-MSL maleimide spin label. Temperature: 210 K. ED spectra are recorded for interpulse spacings of (top to bottom) $\tau = 168$, 296, and 424 ns. Spectra are corrected for instantaneous diffusion according to eq 3 and are normalized to the central lineheight. Beneath each spectrum is given the anisotropic part of the relaxation rate, W, obtained according to eq 4 from pairs of spectra with interpulse separations of $\tau_1 = 168$ and $\tau_2 = 296$ ns, or $\tau_1 = 168$ and $\tau_2 = 424$ ns.

exponential. At low temperatures, below 150 K, a biexponential fit is superior to a single exponential fit, indicating a heterogeneous distribution of phase-memory times (see, e.g., Figure 4). The difference between the phase-memory times of the two components decreases progressively with increasing temperature in the low-temperature regime. Then, at temperatures above 150 K, the echo decays become single exponential, corresponding to a single phase-memory time at a given temperature for each sample. In this high-temperature regime, the phase memory times are shorter for class I groups than for class II groups, reflecting the difference in environment of the two classes of −SH groups. The phase-memory times of class I groups are shorter for the pig enzyme than those for the shark enzyme, suggesting somewhat different environments in the two enzymes, whereas for class II groups they are very similar for both species. Note that none of the decay curves which are fitted by a biexponential function at low temperatures can be described by a stretched exponential with τ-exponent greater than unity (cf. refs *21*−*24*).

Whereas the heterogeneity of phase-memory times might arise from different sites of labeling on the same protein, this in no way accounts for finding a single unique phase-memory time for all sites within a given class at any particular temperature above 150 K. This highly significant result arises from the transition to a regime in which the spin-labeled enzymes are no longer restricted to different (possibly local) substates. Environmental differences between class I and class II groups, and between class I groups of shark and pig enzymes, are nevertheless preserved. The latter findings suggest that heterogeneity of substates is a global property of the enzyme ensemble, rather than representing local differences in a single enzyme molecule.

Two-Pulse, Primary Echo-Detected EPR Spectra. Figure 5 shows the two-pulse, echo-detected (ED) EPR spectra of Na,K-ATPase preparations spin-labeled on class I (upper panel) or class II (lower panel) −SH groups with 5-MSL. Spectra from shark membranes are given on the left and those from pig are given on the right. The spectra are recorded at 210 K and are

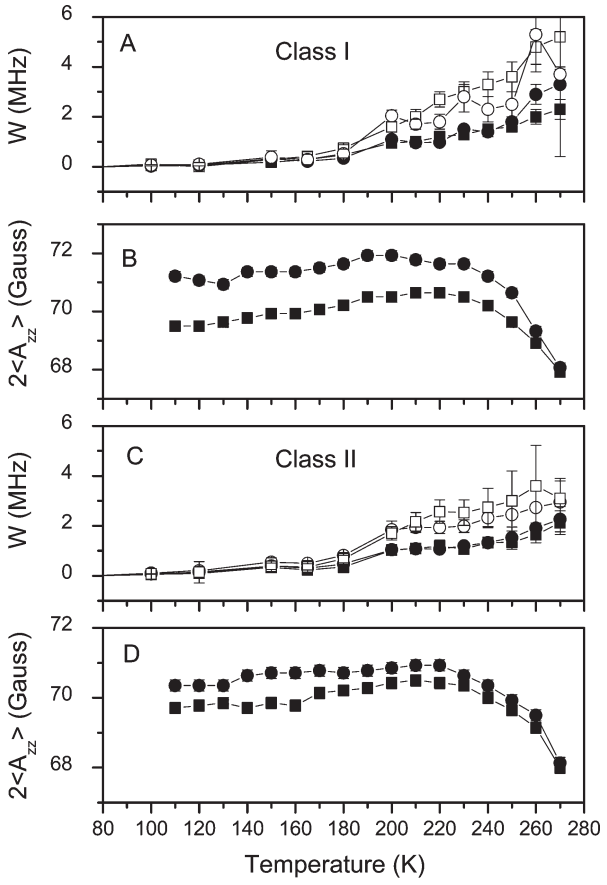

FIGURE 6: Temperature dependence of the W_L (solid symbols) and W_H (open symbols) ED-EPR relaxation-rate parameters of class I (A) and class II (C) groups, and of the outer hyperfine splitting, $2\langle A_{zz}\rangle$, in the CW-EPR spectra of class I (B) and class II (D) groups, for 5-MSL-labeled shark (circles) and pig (squares) Na,K-ATPase.

given for various values of the echo delay time τ. They have been corrected for instantaneous diffusion according to eq 3 by using spectra recorded at 77 K. The dependence of the ED-lineshapes on the τ-delay reveals preferential relaxation in the intermediate spectral regions at low- and high-field that is characteristic of rapid, small-amplitude torsional librations (*25*, *26*). The corresponding relaxation spectra, as defined by eq 4, are given underneath the ED spectra in Figure 5. *W*-Relaxation spectra evaluated for different pairs of τ_1 and τ_2 coincide to within the noise level, showing that the relaxation is close to exponential. This is consistent with the so-called "isotropic" model for librational dynamics, in which uncorrelated librational motions take place simultaneously about the nitroxide *x*-, *y*-, and *z*-axes, but not with those for uniaxial libration (*19*).

Figure 6A shows the temperature dependence of the *W*-relaxation parameter for spin-labeled class I groups; corresponding data for class II groups are given in Figure 6C. The *W*-relaxation parameter is calculated from intensity ratios in the low- and high-field intermediate regions (W_L and W_H, respectively) as defined in Figure 5, for two fixed delay times $\tau_1 = 168$ ns and $\tau_2 = 296$ ns. This parameter is determined by the product of the mean-square torsional amplitude $\langle\alpha^2\rangle$, and the librational correlation time, τ_c (*19*). The temperature profiles of W_L (solid symbols) and W_H (open symbols) are very similar, in each case, showing consistency between the low- and high-field regions of the ED spectra. The two profiles can be brought into numerical accord by multiplying the absolute values of W_L by a factor of approximately 1.7× for shark and 2.0× for pig Na,K-ATPase. In each case, the librational intensity remains very low up to ca. 180 K, increases sharply to 200 K, and then increases less steeply with further increase in temperature. Rather similar results are obtained for shark and pig class II groups and also pig class I groups. At the highest temperatures (≥260 K), the *W*-relaxation rate for shark class I groups is, however, greater than for the other three cases.

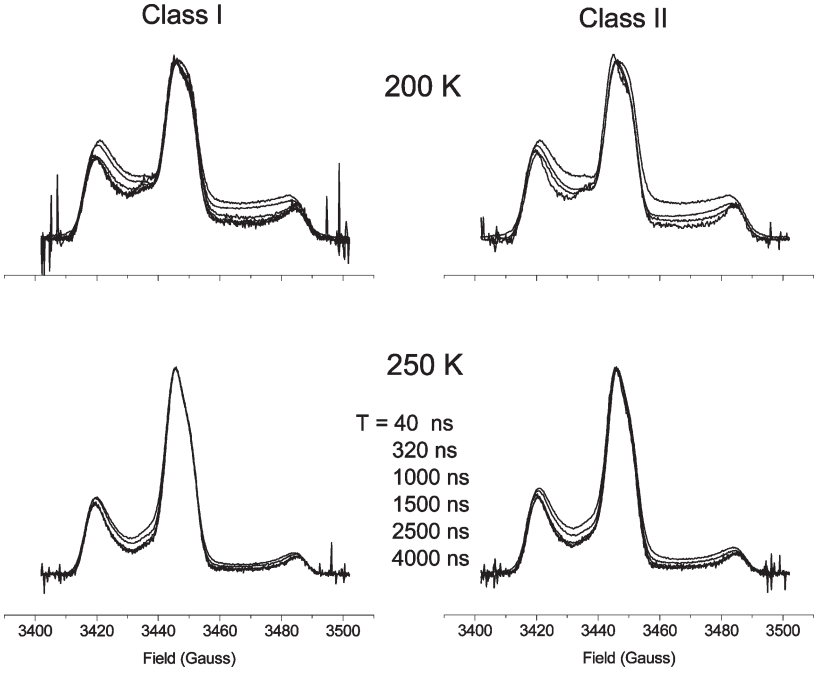

FIGURE 7: Three-pulse, stimulated-echo ED-EPR spectra of shark Na,K-ATPase membranes that are labeled on class I (left-hand side) or class II (right-hand side) −SH groups with 5-MSL. Temperature: 200 K (upper row) and 250 K (lower row). ED spectra are recorded for fixed $\tau = 216$ ns and increasing *T*-delay (top to bottom), as indicated. Spectra are corrected for spin−lattice relaxation according to eq 5 by using inversion−recovery ED-EPR spectra recorded at the same temperature, and are normalized to the central lineheight.

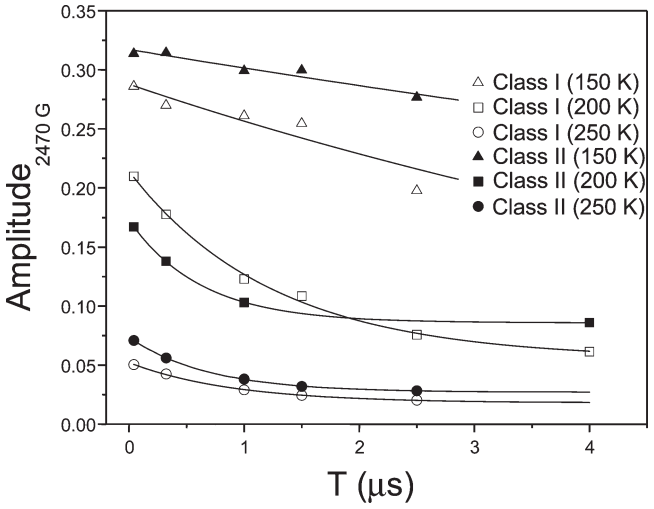

FIGURE 8: Dependence on T-delay of the amplitude at 3470 G field position ($m_I = -1$ manifold) from three-pulse ED-EPR spectra of shark Na,K-ATPase membranes that are labeled on class I (open symbols) or class II (solid symbols) −SH groups with 5-MSL. The first interpulse delay is maintained fixed at $\tau = 168$ ns. Temperature: 150 K (triangles), 200 K (squares) and 250 K (circles). Solid lines are single exponential fits according to eq 11.

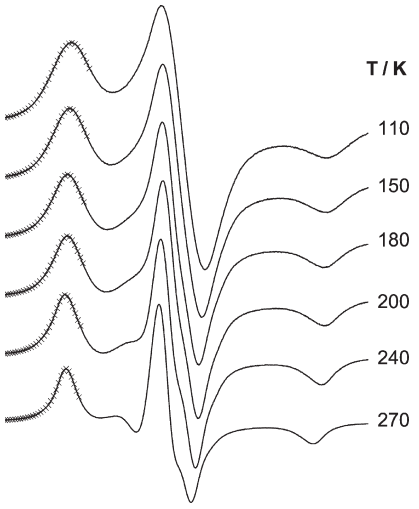

FIGURE 9: Temperature dependence of the CW-EPR spectra of 5-MSL-labeled class II −SH groups of shark Na,K-ATPase. Crosses represent fitting of the low-field ($m_I = +1$) hyperfine extremum with a Voigt line shape (eq 6). Total scan width = 100 G.

Table 1: Correlation times, τ_c^*, for slow motion obtained from exponential T-dependences of three-pulse ED_{SE} spectra from shark Na,K-ATPase spin-labeled with 5-MSL on Class I or Class II −SH groups[a]

	τ_c^* (μs)		
−SH groups	150 K	200 K	250 K
class I	9 ± 2	1.26 ± 0.12	0.91 ± 0.06
class II	20 ± 2	0.62 ± 0.01	0.69 ± 0.02

[a]Single-exponential fitting according to eq 11.

The two-pulse ED spectra therefore indicate that a glasslike transition occurs in the librational dynamics of the protein at around 200 K. This is a general feature of the membranous Na,K-ATPase protein, insofar as it is found for both shark and pig enzymes, and refers to the torsional dynamics of both class I and class II spin-labeled cysteine residues. The method is directly applicable to study glass transitions in other large membrane-bound proteins.

Three-Pulse, Stimulated Echo-Detected EPR Spectra. Three-pulse, stimulated-echo ED-EPR spectra are sensitive to motions on the time scale of spin−lattice relaxation (T_1), which is much longer than the phase-memory time (T_{2M}) that determines the time-scale for two-pulse, primary echo ED-EPR (*18*, *27*). Figure 7 shows the three-pulse ED-EPR spectra of shark Na,K-ATPase preparations spin-labeled on class I (left) or class II (right) −SH groups with 5-MSL. The spectra are recorded at 200 or 250 K and are given for various values of the second delay time, T. They have been corrected for spin−lattice relaxation during the T-delay by using inversion recovery measurements, according to eq 5. The dependence of the stimulated ED-lineshapes on the T-delay reveals preferential relaxation in the intermediate spectral regions at low- and high-field, as for the two-pulse ED spectra, but on the microsecond time scale instead of the nanosecond time scale (see ref *18*).

Figure 8 shows the T-dependence of the ED_{SE}^{norm} spectral amplitude at the center of the high-field manifold (B = 3470 G). This corresponds to the spectral position that is most sensitive to the angular dynamics. In each case, the high-field amplitude is normalized to the central line height, which is largely insensitive to angular-dependent changes. (Note that this normalization largely suppresses the sensitivity of the stimulated echo decay to nuclear spin relaxation of the rotating methyl groups (*28*)). Least-squares fitting, shown in Figure 8, yields single-exponential decay times, τ_c^*. (An asterisk is used to distinguish the correlation times of the slow motions detected in three-pulse ED-EPR from those of the rapid librations in two-pulse ED-EPR.) The values of these single decay times at 200 and 250 K are given in Table 1. They are all in the microsecond regime and are longer for class I groups than for class II groups.

Stimulated-echo experiments were also performed at 150 K, which is just below the glasslike transition that is detected by the onset of rapid librational dynamics to which the two-pulse echo-detected spectra are sensitive. The normalized ED_{SE} lineheight at 3470 G is greater at 150 K than at the higher temperatures (see Figure 8) and, in relative terms, decreases more slowly with increasing delay time T. The effective decay times, which are included in Table 1, are much longer than those at 200 K. Thus, on both the nanosecond and microsecond time scales, a glasslike transition occurs in the protein dynamics. The longer time scale of the changes to which the ED_{SE} spectra are sensitive indicates that the dynamic transition is not restricted to librations alone but extends also to larger scale, more cooperative motions. The latter motions must involve appreciable sections of the protein and therefore are suitable candidates to be on-pathway in the enzymatic cycle. That the glasslike transition involves such large-scale motions suggests that the substates whose activation barriers are traversed correspond to a heterogeneous protein ensemble rather than to local heterogeneities within a given protein.

Continuous Wave (CW) EPR Spectra. Conventional CW spectra of the shark and pig Na,K-ATPase preparations that were spin-labeled on class I or class II −SH groups were also recorded as a function of temperature, in order to determine the angular amplitude, α, of librational motion at higher temperatures and the conformational heterogeneity that may be frozen in at lower temperatures. Figure 9 shows the temperature dependence of typical CW-EPR spectra from 5-MSL-labeled Na,K-ATPase, in this case from class II −SH groups of the

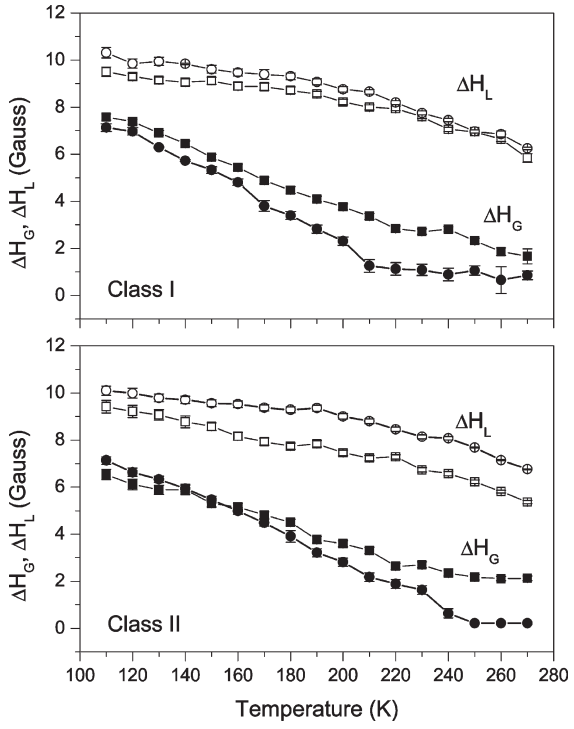

FIGURE 10: Temperature dependence of the deconvoluted Gaussian (ΔH_G, solid symbols) and Lorentzian (ΔH_L, open symbols) widths of the low-field ($m_I = +1$) hyperfine line obtained by fitting Voigt lineshapes (eq 6) to the CW-EPR spectra of 5-MSL-labeled class I (upper panel) or class II (lower panel) −SH groups of shark (circles) and pig (squares) Na,K-ATPase.

shark enzyme. The powder patterns obtained at low temperature are characterized by extremely broad lines with inhomogeneously broadened lineshapes of pronounced Gaussian character. With increasing temperature, the lines narrow progressively and the lineshapes become more homogeneous until finally they become almost purely Lorentzian in character. The crosses in Figure 9 represent fitting of a Voigt absorption line shape (eq 6) to the low-field hyperfine extremum. This latter line shape corresponds to a Gaussian convolution of pure Lorentzian components.

Figure 10 shows the temperature dependences of the widths of the Gaussian distribution (ΔH_G) and of the Lorentzian components (ΔH_L) that are obtained by fitting the CW-EPR spectra of class I and class II groups of the shark and pig Na,K-ATPases (cf. Figure 9). The Lorentzian linewidths decrease only slowly up to 200 K and then decrease gradually with further increase in temperature. In contrast, the widths of the Gaussian distributions decrease progressively already from the lowest temperatures, reaching zero or rather low values at temperatures above 220 K. This corresponds to averaging of the inhomogenous broadening by exchange processes (cf. (*29*)).

The temperature dependences of the outer hyperfine splitting, $2\langle A_{zz}\rangle$, for both shark and pig preparations spin-labeled on class I groups are shown in Figure 6B; corresponding data for class II −SH groups are given in Figure 6D. For class I groups at low temperatures, values of $\langle A_{zz}\rangle$ for the shark enzyme are considerably larger than those for the pig enzyme (Figure 6B), indicating a higher environmental polarity for the former (see, e.g., refs *30*, *31*). In contrast, the corresponding values for shark and pig class II groups are much more comparable. Initially, the effective hyperfine splittings increase slightly with increasing temperature. This is associated with the conformational heterogeneity at low temperature, which is evidenced by the inhomogeneous

Table 2: Normalized Intensities of the Total (I_{tot}) and Broad (I_{broad}) Components in the ^{2}H-ESEEM Spectra, and Rigid-Limit Hyperfine Coupling (A_{zz}) in the CW-EPR Spectra, from Shark and Pig Na,K-ATPase Spin-Labeled with 5-MSL on Class I or Class II −SH Groups

−SH groups	I_{tot} (ns)	I_{broad} (ns)	I_{broad}/I_o[a]	A_{zz} (G)
		Class I		
shark	210	86	0.76	35.9 ± 0.1
pig	151	62	0.55	35.3 ± 0.1
		Class II		
shark	157	64	0.56	35.5 ± 0.1
pig	156	64	0.56	35.3 ± 0.1

[a] I_o is the theoretical intensity for one D_2O hydrogen bonded to a nitroxide (*16*).

(i.e., Gaussian) broadening that is shown in Figure 10. At around 200 K, the splittings reach their maximum value and remain approximately constant until 220 K. Under these conditions, the Gaussian linewidths are greatly reduced relative to lower temperatures, and the splittings correspond to their rigid-limit values, $2A_{zz}$. These latter polarity-dependent indices are listed together with the D_2O-ESEEM data in Table 2.

Above 220 K, the values of $2\langle A_{zz}\rangle$ decrease continuously with increasing temperature, as a result of progressive motional narrowing by the rapid, small-angle torsional librations (*32*). In this dynamic regime, values of $2\langle A_{zz}\rangle$ for shark class I groups are greater than those for the pig enzyme (Figure 6B), whereas for class II groups the values are more similar for the two ATPases (Figure 6D).

Characterization of Librational Motion. Figure 11A shows the temperature dependence of the librational amplitude−correlation time product, $\langle\alpha^2\rangle\tau_c$, for shark and pig Na,K-ATPase labeled on class I or class II −SH groups. These values are obtained from the pulse-EPR measurements of W_L that are given in Figures 6A and 6C, by using a conversion factor relating $\langle\alpha^2\rangle\tau_c$ to W_L of 1.0×10^{17} rad^{-2} s^{-2}. A calibration factor with this value was established previously, both for alamethicin spin-labeled with TOAC and a phospholipid spin-labeled in the lipid chain, by using spectral simulations with the "isotropic" librational model (*19*, *33*).

Figure 11B shows the temperature dependence of the mean-square amplitude, $\langle\alpha^2\rangle$, of the librational motion for the two Na,K-ATPases labeled on class I or class II −SH groups. These values are derived from the motionally averaged hyperfine splittings in Figures 6B and 6D, according to (*32*)

$$\langle A_{zz}\rangle = A_{zz} - (A_{zz} - A_{xx})\langle\alpha^2\rangle \quad (7)$$

where the angular brackets indicate a motionally averaged hyperfine tensor (of principal elements A_{xx}, A_{yy} and A_{zz}). From 200 K upward, the temperature dependence of the librational amplitude is very similar for shark and pig class II groups, and also pig class I groups. It is very small up to 220 K and then increases rapidly with increasing temperature. For shark class I groups, the amplitude is significantly larger at higher temperatures than in the other three cases. The largest value of $\langle\alpha^2\rangle$ recorded in Figure 11B corresponds to a root-mean-square amplitude of 12° for both shark and pig preparations (14° for shark class I groups) at 270 K, which confirms that the small-amplitude approximation is appropriate over the temperature range studied.

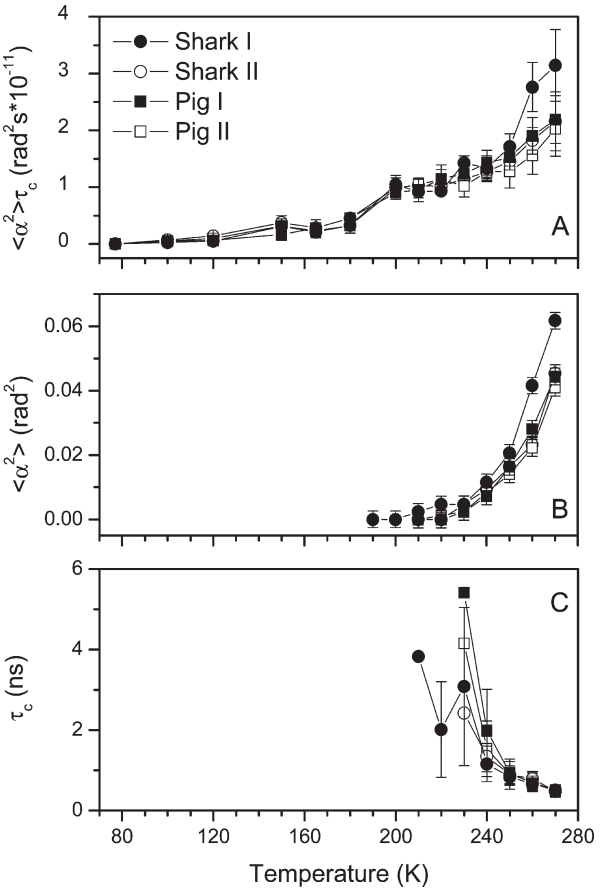

FIGURE 11: Temperature dependence of (A) the amplitude−correlation time product, $\langle\alpha^2\rangle\tau_c$ (values are obtained from measurements of the W_L relaxation-rate parameter—see Figure 6); (B) the librational amplitude, $\langle\alpha^2\rangle$ (values are obtained from the motionally averaged hyperfine splitting, $2\langle A_{zz}\rangle$, together with eq 7); and (C) the librational correlation time, τ_c (values are obtained from the amplitude−correlation product in part A and the librational amplitude in part B). Shark (circles) or pig (squares) Na,K-ATPase membranes are spin-labeled with 5-MSL on class I (solid symbols) or class II (open symbols) −SH groups.

Figure 11C shows the temperature dependence of the rotational correlation time, τ_c, for the librational motion of shark and pig Na,K-ATPase labeled on class I or class II −SH groups. Determinations of the amplitude−correlation time product, $\langle\alpha^2\rangle\tau_c$, from Figure 11A are combined with the amplitude (i.e., $\langle\alpha^2\rangle$) measurements that are given in Figure 11B to obtain these values for τ_c. Evaluations are possible only at temperatures above 220 K, for which $\langle\alpha^2\rangle$ is nonzero. Correlation times at temperatures above 240 K are in the subnanosecond regime, appropriate to rapid small-amplitude librations, and are essentially identical for all systems. They decrease relatively rapidly with increasing temperature up to 250 K, and beyond this the temperature dependence is still appreciable. Apparently, libration is an activated process in this temperature regime.

Thus, rapid librational motion becomes appreciable at the temperatures required for crossing the activation barriers that separate conformational substates. Quite possibly such librational motions provide the thermal fluctuations that drive the intersubstate conformational exchange. They are a general dynamic phenomenon, found in both shark and pig enzymes, and with similar amplitudes and rates except for the larger amplitude of shark class I groups. Qualitatively similar behavior can be expected in other large membrane-spanning proteins.

Table 3: Fractions of Spin-Labeled Class I and Class II −SH Groups in Shark or Pig Na,K-ATPase That Are Hydrogen Bonded by One (f_{1W}) and Two (f_{2W}) Water Molecules, and Product of the Equilibrium Constant for H-Bonding, K, with the Effective Free Water Concentration, [W], from ^{2}H-ESEEM Spectra of D_2O-Membrane Dispersions[a]

−SH groups	K[W]	f_{1W}	f_{2W}
	Class I		
shark	0.61	0.47	0.14
pig	0.38	0.40	0.07
	Class II		
shark	0.39	0.40	0.08
pig	0.39	0.40	0.08

[a]Values deduced from eqs 8−10.

DISCUSSION

As discussed below, spin-labeled Na,K-ATPase provides an excellent system on which to determine the potential of different pulse-EPR techniques for investigating multiple, well-characterized cysteine sites. In addition, combining this with quantifying inhomogeneous broadening in the conventional CW-EPR spectra affords a new method to study the heterogeneity of conformational substates in proteins. This work also considerably extends such studies by addressing a complex, membrane-bound transport system, rather than the relatively small soluble or crystalline proteins investigated previously. The potential biochemical significance of conformational fluctuations between substates is well recognized (*9*) and is found here to apply also to membrane enzymes.

Classification of −SH groups. Class I and class II −SH groups of shark Na,K-ATPase are distinguished operationally by their reactivity with maleimide (*3*, *4*). Here, we find that the accessibility to water (which is analyzed in more detail below) is greater for shark class I groups than for shark class II groups (see Table 2). This is in agreement with the higher reactivity toward NEM, and with the higher polarity that is indicated by conventional EPR in Figure 6. A difference between pig class I and class II groups is found in the phase-memory time, T_{2M}, of the 5-MSL-labeled enzyme at temperatures in the homogeneous region above 150 K (see Figure 3). This latter illustrates how pulse-EPR techniques, additional to D_2O-ESEEM, can be used to distinguish the environments of different classes of −SH residues in a complex membrane enzyme.

In terms of the enzyme structure (see Figure 1), it is likely that the class I groups are located in the cytoplasmic region, and that at least part of the class II groups reside in the transmembrane region. This is reflected in the accessibility to water that is defined unambiguously by D_2O-ESEEM spectroscopy. The class II group that is protected from labeling in the presence of ATP and K^+ is probably that close to the nucleotide binding site (Cys^{428} in shark and Cys^{421} in pig). Approximately 60% of the spin intensity of class II groups remains membrane-associated after trypsinization (*34*). Therefore, these constitute part of the groups depicted in the right-hand panel of Figure 1, and the remainder most likely contribute to those in the left-hand panel.

Water Accessibility. DFT calculations predict that the normalized ^{2}H-ESEEM intensity for a nitroxide with a single hydrogen-bonded D_2O molecule is $I_o \approx 115$ ns (*16*). From the intensities, I_{broad}, of the broad D_2O-ESEEM component in Table 2, it is therefore estimated that approximately 56% of

the spin-labeled class II −SH groups on both shark and pig Na,K-ATPase are H-bonded to water. A similar percentage is obtained for spin-labeled class I groups on pig Na,K-ATPase, but for the shark enzyme the fraction of H-bonded class I groups is considerably higher (76%). These results correlate well with measurements of the polarity dependent rigid-limit hyperfine coupling, A_{zz}, which are included in Table 2. The values of A_{zz} are very similar for shark and pig spin-labeled class II groups and pig class I groups, whereas that for spin-labeled shark class I groups is larger, corresponding to a higher average environmental polarity for the latter (see, e.g., ref *35*).

By application of the mass-action law, the product of the equilibrium constant, K, for H-bonding and the effective concentration, [W], of free water is related to the normalized intensity of the broad D_2O-ESEEM component by (*16*)

$$K[\mathrm{W}] = \frac{I_{\mathrm{broad}}/I_{\mathrm{o}}}{2 - I_{\mathrm{broad}}/I_{\mathrm{o}}} \tag{8}$$

Correspondingly, the fraction of spin-labeled −SH groups that are H-bonded by a single water molecule is given by (*16*)

$$f_{1\mathrm{W}} = \frac{2}{1/K[\mathrm{W}] + 2 + K[\mathrm{W}]} \tag{9}$$

The fraction of spin-labeled −SH groups that are H-bonded by two water molecules is then given by

$$f_{2\mathrm{W}} = \frac{1}{2}\left(\frac{I_{\mathrm{broad}}}{I_{\mathrm{o}}} - f_{1\mathrm{W}}\right) \tag{10}$$

Table 3 lists the values of K[W], f_{1W} and f_{2W} that are obtained for class I and class II groups in shark and pig Na,K-ATPases. For comparison, the values that are obtained with spin-labeled lipids in bilayer membranes of dipalmitoyl phosphatidylcholine + 50 mol % cholesterol are K[W] = 0.31, with fraction of nitroxides H-bonding to one water of $f_{1W} = 0.36$, and fraction H-bonding to two waters of $f_{2W} = 0.06$, at the C4 position of the *sn*-2 chain. These values fall to zero at the C14 position, where the transition between the upper and lower regions takes place at around the C8 chain position (*16*). For fatty acid chains in the hydrophobic binding site of human serum albumin, the corresponding values vary between K[W] = 0.28 and 0.54, $f_{1W} = 0.34$ and 0.46, and $f_{2W} = 0.05$ and 0.12, at the C7 and C16 positions, respectively, of stearic acid (*20*). On the other hand, for 5-MSL bound covalently at the surface of HSA, which corresponds to maximum water exposure, the higher values of K[W] = 0.64, f_{1W} = 0.48 and $f_{2W} = 0.15$ are obtained. The 5-MSL-labeled class I −SH groups of shark Na,K-ATPase therefore are comparably hydrated to a surface-exposed −SH group on a water-soluble protein. The extent of hydration of Na,K-ATPase class II −SH groups of both shark and pig, and of pig class I −SH groups, is considerably smaller, although greater than that of the most buried fatty acid chain segments in the hydrophobic binding site of HSA and the 4-C atom chain position toward the polar headgroups in cholesterol-containing phospholipid bilayers. It corresponds to an intermediate degree of burial for the fatty acid chain segments in the HSA binding pocket. Pulsed-EPR determinations of water-accessibility therefore correspond very well with what is known about the different classes of −SH groups in spin-labeled Na,K-ATPase, and illustrate the depth of detail that can be achieved by using ESEEM spectroscopy of D_2O.

Librations and Conformational Substates. The CW-EPR lineshapes indicate conformational heterogeneity in the low-temperature regime. This microheterogeneity is characterized by a Gaussian distribution of substates with different effective A_{zz}-hyperfine couplings and possibly also different spin−spin interactions with any neighboring nitroxide (see Figures 9 and 10). At temperatures above approximately 220 K, where the amplitude of the rapid librational motions becomes appreciable (Figure 11B), the Gaussian distribution width is reduced to zero, or a rather small value (Figure 10), and the enzyme molecules are no longer restricted to a particular substate. Qualitatively, this behavior is mirrored by the phase-memory relaxation times, T_{2M}. At low temperatures, the echo decay curves are characterized by more than one relaxation time, whereas at higher temperatures (above approximately 150 K) they can be described by a single exponential decay (Figures 3 and 4).

To achieve dynamic averaging of the inhomogeneous broadening, the rate of exchange ($k_{ex} = k_{+1} + k_{-1}$, where k_{+1} and k_{-1} are the on- and off-rates) between the conformational substates must be considerably greater than the intrinsic Gaussian line width, $\Delta H^{\circ}_{G} \approx 30$ MHz (see Figure 10 and, e.g., ref *36*). If the GHz-range librational motions seen by the ED spectra (Figure 11) are identified with the frequency factor in absolute rate theory, then exchange rates exceeding 30 MHz would imply modest activation barriers of 6 kJ mol^{-1}, or less, between conformational substates. Exchange at these rates is expected to give a contribution to the Lorentzian linebroadening of $\delta\Delta H_L \approx (1 - f_{conf})f_{conf}(\Delta H^{\circ}_{G})^2/k_{ex}$, where f_{conf} is the fractional population of one of the two substates between which exchange takes place. This value is therefore considerably less than ΔH°_{G}, which is consistent with the relatively small temperature dependence of ΔH_L that is seen in Figure 10.

Three-pulse ED_{SE} spectra at temperatures of 200 K or higher (see Figure 7) demonstrate that conformational exchange also occurs on a time scale much slower than that considered above, in the region of 1 MHz or less. For a simple two-site, slow-exchange model, the amplitude of the stimulated echo is given by (*18*, *37*)

$$E(2\tau + T, \Delta\omega) = \frac{1}{2}\exp\left(-\frac{\tau}{\tau_c^*}\right)\left[(1 - \cos\Delta\omega\tau)\exp\left(-\frac{T}{\tau_c^*}\right) + 1 + \cos\Delta\omega\tau\right] \tag{11}$$

where $\Delta\omega$ is the difference in angular resonance frequency between the two states, and $(2\tau_c^*)^{-1}$ is the rate of exchange between states. The exchange rates that are implied by the stimulated-echo data of Table 1 are therefore in the region of 0.4−0.8 MHz at 200 K and above. This corresponds to a slower exchange than that averaging the heterogeneity of substates, which is found at temperatures below 200 K, and likely corresponds to less localized conformational changes than the former. Quite possibly, a whole range of hierarchies of conformational exchange rates may exist in a protein of the complexity of Na,K-ATPase, extending up to those limiting enzyme turnover. NMR studies of T_2-relaxation, mostly on soluble enzymes, have demonstrated exchange between conformational substates that is on the μs to ms time scale (ref *38* and references therein). In the case of the longer time scales, global exchange processes are found to correspond with rate-limiting conformational changes between major enzyme intermediates. The faster exchange processes found here in the Na,K-ATPase by EPR correspond to different degrees of ruggedness in the conformational landscape that could lie on-pathway between the major conformational states.

Thus, the region below 200 K is characterized by inhomogeneously broadened lines in the CW-EPR spectra, heterogeneity in the phase-memory times, and very little *W*-relaxation in the ED spectra. This arises from freezing-in of the protein in heterogeneous substates. At around 200 K, the system undergoes a glasslike transition to a state in which the CW-EPR spectra have homogeneous narrow lines, the spin echo decays with a single phase-memory time, and *W*-relaxation of the ED spectra indicates the onset of rapid small-amplitude libration. This is similar to the behavior of soluble proteins in this temperature region. A variety of evidence, such as kinetic, diffraction, neutron scattering and Mössbauer, suggests that below about 200 K a protein is frozen into a particular conformational substate, and above this temperature the protein fluctuates from substate to substate (*9*). Whereas this dynamic transition in soluble proteins appears to be coupled to a glass transition in the hydration water (*10*), the transition at 200 K in the hydration layer of the purple membrane does not drive a corresponding dynamic transition in the bacteriorhodopsin protein (*39*). Our present results indicate that the Na,K-ATPase behaves more like the soluble proteins than like bacteriorhodopsin, which is a highly hydrophobic protein that is embedded almost entirely within the lipid membrane. Conceivably the conformational substates in Na,K-ATPase, including those corresponding to the microsecond exchange processes probed by three-pulse ED-EPR, are involved in the pathway between the different principal conformations, E_1ATP, E_1P, E_2P and $E_2(K)$, that are involved in the enzymatic cycle of P-type ATPases (see, e.g., ref *40*). The ED spectra from pulsed-EPR of spin-labeled proteins are therefore able to identify those dynamic fluctuations that drive transitions between substates in the conformational landscape of membrane enzymes.

CONCLUSIONS

Large eukaryotic membrane proteins of the complexity and physiological significance of the Na,K-ATPase are not readily amenable to high levels of expression in recombinant form, in contrast to the situation for prokaryotic proteins. Hence, biophysical studies must be made mostly with the native protein; in the case of spin-labeling this means with the native complement of cysteine residues. Biochemical methods, in terms of labeling and inactivation kinetics, allow some discrimination between different −SH groups. Here, it is shown that D_2O-ESEEM spectroscopy provides detailed information on the differences in environmental polarity and accessibility to water of Na,K-ATPase class I and class II groups, and of the differences between shark and pig enzyme class I groups (the more membrane-buried class II groups are similar for both). The phase-memory times from spin−echo decays also discriminate between class I and class II groups of the pig enzyme. This application to the Na,K-ATPase illustrates the level of detail that might be achieved with other proteins of comparable complexity when applying these pulse-EPR techniques.

Both phase-memory times and CW-EPR lineshapes reveal that the spin-labeled protein populates an ensemble of heterogeneous conformational substates at low temperatures, but interconverts between these substates at higher temperatures, above ca. 200 K. Heterogeneity of substates is likely a global property of the enzyme ensemble, independent of multiple labeling, because differences in dynamics between class I and class II groups, and between shark and pig enzymes, are still found when the substates are uniformly populated. There are distinct parallels with the global conformational behavior of soluble proteins, as studied by neutron scattering and Mössbauer spectroscopy. The biochemical implications of these results are similar to those already advanced in the latter cases (*9*).

The onset of rapid librational motions and larger-scale microsecond motions (detected by two-pulse and three-pulse ED-spectroscopy, respectively) occurs at temperatures corresponding to interconversion between conformational substates. Relatively modest activation barriers for interconversion are implied. The larger-scale motions must be partially cooperative in nature and are part of a range of conformational exchange rates that involve a hierarchy of substates that ultimately lie on the pathway of the enzymatic cycle of the sodium pump.

ACKNOWLEDGMENT

We thank Ms. Angelina Damgaard for excellent technical assistance. R.G., R.B., L.S. and D.M. are members of the COST P15 Action of the European Union.

REFERENCES

1. Morth, J. P., Pedersen, B. P., Toustrup-Jensen, M. S., Sørensen, T. L.-M., Petersen, J., Andersen, J. P., Vilsen, B., and Nissen, P. (2007) Crystal structure of the sodium-potassium pump. *Nature 450*, 1043–1050.
2. Esmann, M., Hideg, K., and Marsh, D. (1992) Analysis of thiol-topography in Na,K-ATPase using labelling with different maleimide nitroxide derivatives. *Biochim. Biophys. Acta 1112*, 215–225.
3. Esmann, M. (1982) Sulfhydryl groups of (Na^++K^+)-ATPase from rectal glands of *Squalus acanthias* - titration and classification. *Biochim. Biophys. Acta 688*, 251–259.
4. Esmann, M. (1982) Sulfhydryl groups of (Na^++K^+)-ATPase from rectal glands of *Squalus acanthias*: detection of ligand induced conformational changes. *Biochim. Biophys. Acta 688*, 260–270.
5. Fahn, S., Hurley, M. R., Koval, G. J., and Albers, R. W. (1966) Sodium-potassium-activated adenosine triphosphatase of *Electrophorus* electric organ. II. Effects of *N*-ethylmaleimide and other sulfhydryl reagents. *J. Biol. Chem. 241*, 1890–1895.
6. Wallick, E. T., Anner, B. M., Ray, M. V., and Schwartz, A. (1978) Effect of temperature on phosphorylation and ouabain binding to *N*-ethylmaleimide-treated (Na^+,K^+)-ATPase. *J. Biol. Chem. 253*, 8778–8786.
7. Esmann, M., Klodos, I. (1983) Sulfhydryl groups of Na,K-ATPase: Effects of *N*-ethylmaleimide on phosphorylation from ATP in the presence of Na^+ + Mg^{2+}, in Structure, Mechanism and Function of the Na/K-Pump (Hoffman, J. F., Forbush, B., III, Eds.) pp 349−352, Academic Press, New York.
8. Bartucci, R., Erilov, D. A., Guzzi, R., Sportelli, L., Dzuba, S. A., and Marsh, D. (2006) Time-resolved electron spin resonance studies of spin-labelled lipids in membranes. *Chem. Phys. Lipids 141*, 142–157.
9. Frauenfelder, H., Parak, F., and Young, R. D. (1988) Conformational substates in proteins. *Annu. Rev. Biophys. Biophys. Chem. 17*, 451–479.
10. Doster, W. (2008) The dynamical transition of proteins, concepts and misconceptions. *Eur. Biophys. J. 37*, 591–602.
11. Klodos, I., Esmann, M., and Post, R. L. (2002) Large-scale preparation of sodium-potassium ATPase from kidney outer medulla. *Kidney Int. 62*, 2097–2100.
12. Skou, J. C., and Esmann, M. (1979) Preparation of membrane-bound and of solubilized (Na^++K^+)-ATPase from rectal glands of *Squalus acanthias*. The effect of preparative procedures on purity, specific and molar activity. *Biochim. Biophys. Acta 567*, 436–444.
13. Jørgensen, P. L. (1974) Purification and characterization of (Na^++K^+)-ATPase. III. Purification from the outer medulla of mammalian kidney after selective removal of membrane components by sodium dodecyl sulphate. *Biochim. Biophys. Acta 356*, 36–52.
14. Lowry, O. H., Rosebrough, N. J., Farr, L., and Randall, R. J. (1951) Protein measurement with the Folin phenol reagent. *J. Biol. Chem. 193*, 265–275.
15. Esmann, M. (1988) ATPase and phosphatase activity of the Na^+,K^+-ATPase; molar and specific activity, protein determinations. *Methods Enzymol. 156*, 105–115.

16. Erilov, D. A., Bartucci, R., Guzzi, R., Shubin, A. A., Maryasov, A. G., Marsh, D., Dzuba, S. A., and Sportelli, L. (2005) Water concentration profiles in membranes measured by ESEEM of spin-labeled lipids. *J. Phys. Chem. B 109*, 12003–12013.
17. Bartucci, R., Guzzi, R., Sportelli, L., and Marsh, D. (2009) Intramembrane water associated with TOAC spin-labelled alamethicin: electron spin-echo envelope modulation by D_2O. *Biophys. J. 96*, 997–1007.
18. Erilov, D. A., Bartucci, R., Guzzi, R., Marsh, D., Dzuba, S. A., and Sportelli, L. (2004) Echo-detected electron paramagnetic resonance spectra of spin-labeled lipids in membrane model systems. *J. Phys. Chem. B 108*, 4501–4507.
19. Erilov, D. A., Bartucci, R., Guzzi, R., Marsh, D., Dzuba, S. A., and Sportelli, L. (2004) Librational motion of spin-labeled lipids in high-cholesterol containing membranes from echo-detected EPR spectra. *Biophys. J. 87*, 3873–3881.
20. De Simone, F., Guzzi, R., Sportelli, L., Marsh, D., and Bartucci, R. (2007) Electron spin-echo studies of spin-labelled lipid membranes and free fatty acids interacting with human serum albumin. *Biochim. Biophys. Acta 1768*, 1541–1549.
21. Klauder, J. R., and Anderson, P. W. (1962) Spectral diffusion decay in spin resonance experiments. *Phys. Rev. 125*, 912–932.
22. Mims, W. B. (1968) Phase memory in electron spin echoes, lattice relaxation effects in $CaWO_4$: Er, Ce, Mn. *Phys. Rev. 168*, 370–389.
23. Hu, P., and Hartmann, S. R. (1974) Theory of spectral diffusion decay using an uncorrelated-sudden-jump model. *Phys. Rev B 9*, 9–13.
24. Lindgren, M., Eaton, G. R., Eaton, S. S., Jonsson, B. H., Hammarstrom, P., Svensson, M., and Carlsson, U. (1997) Electron spin echo decay as a probe of aminoxyl environment in spin-labeled mutants of human carbonic anhydrase II. *J. Chem. Soc., Perkin Trans. 2*, 2549–2554.
25. Dzuba, S. A., Tsvetkov, Yu. D., and Maryasov, A. G. (1992) Echo-detected EPR spectra of nitroxides in organic glasses: model of orientational molecular motions near equilibrium position. *Chem. Phys. Lett. 188*, 217–222.
26. Dzuba, S. A. (1996) Librational motion of guest spin probe molecules in glassy media. *Phys. Lett. A 213*, 77–84.
27. Dzuba, S. A., Kirilina, E. P., Salnikov, E. S., and Kulik, L. V. (2005) Restricted orientational motion of nitroxides in molecular glasses: direct estimation of the motional time scale basing on the comparative study of primary and stimulated electron spin echo decays. *J. Chem. Phys. 122*, 094702−1–094702−7.
28. Kulik, L. V., Salnikov, E. S., and Dzuba, S. A. (2005) Nuclear spin relaxation in free radicals as revealed in a stimulated electron spin echo experiment. *Appl. Magn. Reson. 28*, 1–11.
29. Sachse, J.-H., King, M. D., and Marsh, D. (1987) ESR determination of lipid diffusion coefficients at low spin-label concentrations in biological membranes, using exchange broadening, exchange narrowing, and dipole-dipole interactions. *J. Magn. Reson. 71*, 385–404.
30. Marsh, D. (2002) Polarity contributions to hyperfine splittings of hydrogen-bonded nitroxides - the microenvironment of spin labels. *J. Magn. Reson. 157*, 114–118.
31. Marsh, D., Jost, M., Peggion, C., and Toniolo, C. (2007) Lipid chainlength dependence for incorporation of alamethicin in membranes: EPR studies on TOAC-spin labelled analogues. *Biophys. J. 92*, 4002–4011.
32. Van, S. P., Birrell, G. B., and Griffith, O. H. (1974) Rapid anisotropic motion of spin labels. Models for motion averaging of the ESR parameters. *J. Magn. Reson. 15*, 444–459.
33. Bartucci, R., Guzzi, R., De Zotti, M., Toniolo, C., Sportelli, L., and Marsh, D. (2008) Backbone dynamics of alamethicin bound to lipid membranes: spin-echo EPR of TOAC spin labels. *Biophys. J. 94*, 2698–2705.
34. Esmann, M., Arora, A., Maunsbach, A. B., and Marsh, D. (2006) Structural characterization of Na,K-ATPase from shark rectal glands by extensive trypsinization. *Biochemistry 45*, 954–963.
35. Kurad, D., Jeschke, G., and Marsh, D. (2003) Lipid membrane polarity profiles by high-field EPR. *Biophys. J. 85*, 1025–1033.
36. Horváth, L. I., Brophy, P. J., and Marsh, D. (1988) Exchange rates at the lipid-protein interface of myelin proteolipid protein studied by spin-label electron spin resonance. *Biochemistry 27*, 46–52.
37. Zhidomirov, G. M., and Salikov, K. M. (1969) Contribution to theory of spectral diffusion in magnetically diluted solids. *Sov. Phys. JETP 29*, 1037.
38. Boehr, D. D., Dyson, H. J., and Wright, P. E. (2006) An NMR perspective on enzyme dynamics. *Chem. Rev. 106*, 3055–3079.
39. Wood, K., Plazanet, M., Gabel, F., Kessler, B., Oesterhelt, D., Tobias, D. J., Zaccai, G., and Weik, M. (2007) Coupling of protein and hydration-water dynamics in biological membranes. *Proc. Natl. Acad. Sci. U.S.A. 104*, 18049–18054.
40. Esmann, M., Fedosova, N. U., and Marsh, D. (2008) Osmotic stress and viscous retardation of the Na,K-ATPase ion pump. *Biophys. J. 94*, 2698–2705.